JOURNAL OF THEORETICAL AND APPLIED MECHANICS
46, 2, pp. 413-434, Warsaw 2008

IDENTIFICATION AND SIMULATION OF INITIAL GEOMETRICAL IMPERFECTIONS OF STEEL CYLINDRICAL TANKS

Jarosław Górski
Tomasz Mikulski

Gdańsk University of Technology, Poland
e-mail: jgorski@pg.gda.pl

Critical loads of shell structures can be properly approximated only through including randomness in their geometry. As it is difficult and expensive to measure the initial structure imperfections in situ or in laboratory, a methodology of identification and description of the available data should be provided. The presented procedure provides an opportunity for the reproduction of measured maps of steel cylindrical tank geometrical imperfections. Simulations of nonhomogeneous random fields of imperfections, based on the original conditional-rejection method of simulation, are applied. Using the measured data, an envelope of the imperfections is also estimated. It allows for simulation of extreme but still realistic fields of imperfections. Additionally, nonlinear numerical analyses of tanks with and without initial geometrical imperfections are performed. The results indicate that the initial imperfections influence the solutions.

Key words: cylindrical tanks, geometrical imperfections, random fields, identification and simulation

1. Introduction

Assessment of the reliability, safety and stability of structures with initial material and geometrical imperfections belong to the most complex problems in applied mechanics. The response of a large class of imperfection-sensitive structures (thin shells, thin-walled beams, arches and others) exhibit some features of chaotic systems. Many structural models deal mainly with elastic

stability and include imperfections in a deterministic way, but alternative methods are also implemented. The random nature of the structure behaviour has initiated the use of probabilistic methods (Augusti *et al.*, 1984). Unfortunately, exact analytical solutions to stochastic problems exist only for simple models of structures and uncomplicated cases of loading. To obtain approximate results, a great variety of perturbation techniques and stochastic finite element methods have been developed (see Surdet and Der Kiureghian, 2002; Matthies *et al.*, 1997; Schuëller, 2001). Structure reliabilities are also estimated. For these purposes, the following techniques are in use: the Monte Carlo method, first and second order reliability methods (FORM and SORM), response surface techniques, artificial neural network methods and others (see Hurtado and Barbat, 1998; Marek *et al.*, 1996; Melchers, 1999; Raizer, 2004). When nonlinear geometrical and material effects are taken into consideration, the structure reliability can be evaluated only numerically (Anders and Hori, 1999). But the probabilistic analysis should be used cautiously. For example, it has been demonstrated by Ferson and Ginzburg (1996) what spurious results could be obtained by a stochastic method applied inappropriately.

It is well known that the effect of structural geometrical imperfections can dramatically decrease the nominal load carrying capacity of engineering structures (Arbocz and Starnes, 2002; Khamlichi *et al.*, 2004; Papadopoulos and Papadrakakis, 2004). An analysis of these imperfections can improve the design process (Arbocz, 1998). On the basis of measured and experimental data, the initial structure imperfections can be realistically described by random variables or random fields (Arbocz and Starnes, 2002). An important part of the structural imperfection modelled in a reliability context is the representation of random fields describing the statistical variation of properties or structure parameters. Various attempts have been made to find out ways of doing this (see: Surdet and Der Kiureghian, 2002; Matthies *et al.*, 1997; Vanmarcke, 1983; Vanmarcke *et al.*, 1986; Li and Der Kiureghian, 1993; Zhang and Ellinwood, 1995; Mignolet and Spanos, 1992; Spanos and Mignolet, 1992).

The measured response of a structure, whenever available, should be used to update its reliability. For example, Papadimitriou *et al.* (2001) showed that the structural reliability computed before and after using additional dynamical data could differ significantly. The degree of structure sensitivity to the imperfections depends not only on their magnitude but also on their shape (Arbocz and Starnes, 2002). It is not sufficient to check the shell surface for the maximum imperfection amplitude by carrying out selected circumference or axial measurement scans. A complete surface map of the measured structure should be provided.

The developed methods of the structural data identification are related mainly to dynamical problems (Bendat and Piersol, 1993; Brandt, 1997), and their application to static analysis needs further investigation.

Comprehensive numerical analysis of these problems can be found, for example, in Schenk and Schuëller (2003), where buckling behaviour of cylindrical shells with random geometrical imperfections was examined. A concept of numerical prediction of a large scatter in the limit load observed in experiments using the direct Monte Carlo method, the simulation technique, and the nonlinear finite element method was introduced. The geometric imperfections were modelled as two-dimensional, the Gaussian stochastic process with prescribed second moment characteristics was based on a data bank of measured imperfections. The tests were aided by the Karhunen-Loéve expansion method. Owing to this, it was possible to give the second moment characteristics of the limit load.

Stefanou and Papadrakakis (2004) presented a stochastic triangular shell element in the case of a combined uncertain material (Youngs modulus and the Poisson ratio) and geometrical (thickness) properties. The properties were described by uncorrelated two-dimensional homogeneous fields. The spectral description of the random fields in conjunction with the Monte Carlo simulation was used for the computation variability.

In Papadopoulos and Papadrakakis (2004) by means of the same methodology a parametric study was performed to evaluate the sensitivity of the buckling load of a cylindrical panel to the amplitude and shape of the initial imperfections. One- and two-dimensional stochastic imperfections of shapes, the modulus of elasticity and the shell thickness were introduced individually or in combination. The influence of the shape and magnitude of the imperfections on the form and magnitude of the panel buckling load distributions was investigated. In the case of one-dimensional combined imperfections, a drastical reduction of about 50% of the mean value of the buckling load was observed, whereas in two-dimensional combined imperfections such a reduction was not proved.

The Monte Carlo method combined with the finite element program analysis was also employed by: Bielewicz *et al.* (1994), Walukiewicz *et al.* (1997), Bielewicz and Górski (2002) and Górski (2006). Structural initial imperfections were assumed to be random fields described in terms of a set of simulated realizations and the resulting statistic estimators. This lead to solutions of a set of deterministic problems for the assessment of the structure model responses. The critical load histograms obtained numerically made it possible to estimate the structure reliability. Special attention was paid to discussion

of reduction methods concerning the number of the Monte Carlo realizations. Two methods were considered: the reduction of the initial sets of data, and the accuracy analysis of the output results. An assessment of the structure reliability interval was also proposed.

With regard to compressed cylindrical shells, a reliability based knockdown factor was derived to describe the allowable load applied by Arbocz and Starnes (2002). It can replace the empirical knockdown factor so chosen that when multiplied by the calculated perfect shell buckling load, a "lower bound" relating to all existing experimental data is obtained. But despite some achievements in accurate prediction of the load carrying capacity of an imperfect shell, the problem is still an open question (Papadopoulos and Papadrakakis, 2004).

In this paper, the measured imperfections obtained for steel cylindrical vertical tanks of 5000-50000 m^3 capacity (Orlik, 1976) are considered. An identification procedure and numerical simulation of the initial geometrical imperfections of tanks is proposed. For this purpose a comprehensive statistic analysis of the measured imperfection is provided. To accomplish the numerical simulation, a correlation function describing the imperfection random fields is introduced. In calculations, the conditional-rejection simulation method is used (see Bielewicz *et al.*, 1994; Walukiewicz *et al.*, 1997; Górski, 2006). As the field of initial imperfections is an example of circular data (Fisher, 1993) the simulation method is appropriately modified. The proposed simulation method makes it possible to implement the entire measured data in the calculation process. On this basis a formula which can be used in the prediction of any extreme imperfection in the tank is developed. Additionally, nonlinear numerical analyses of tanks with and without initial geometric imperfections are performed. The results indicate that the initial imperfections influence the solutions.

2. Stochastic description of tank geometric imperfections

A detailed description of in a imperfections steel cylindrical vertical tank can be found in Orlik (1976). Nine sets of measured in situ imperfections of tanks of $V = 5000\text{-}50000\,\mathrm{m}^3$ capacity were analysed (see Table 1, and Fig. 1b-e). The basic statistic parameters of the initial imperfections, i.e. the mean values, standard deviations, and the maximal values are presented in Table 2. It is easy to notice that the discrepancies between the parameters are significant. Examining the shapes of the measured imperfection fields one can describe

them as accidental or even chaotic. Only the first two tank imperfection maps are similar. Even in the case of tanks no. 3 and 4, the dimensions of which are the same as in the first two, the initial imperfections differ evidently. The differences result from tank dimensions, construction method used and precision of the tank assembly. The last reason seems to be the most important. Using the measured data, a procedure of the identification and simulation of the steel tank geometrical imperfection maps is proposed (see also Górski and Mikulski, 2005). Probabilistic methods are applied.

Table 1. Cylindrical vertical tank data (Orlik, 1976)

Tank no.	V [m^3]	Diameter d [m]	Height h [m]	Tank assembly method	Mesh dimension [mm]	Nos. of measureing point	Nos. of points along perim.	Nos. of points along height
1	5000	23.75	11.98	rolled strike	396×750	3232	202	17
2	5000	23.75	11.98	rolled strike	396×750	3232	202	17
3	5000	23.75	11.98	rolled strike	396×750	3030	202	15
4	5000	24.50	11.80	sheets, hand welding	4810×1500	128	16	9
5	13000	36.58	13.45	sheets, hand welding	442×750	168	12	14
6	30000	49.50	16.44	sheets, hand welding	370×1500	3780	420	9
7	30000	49.50	16.44	sheets, hand welding	5981×750	572	26	22
8	32000	54.10	14.40	sheets, hand welding	6060×800	448	28	16
9	50000	65.00	18.01	sheets, automatic	400×1500	5100	510	10

2.1. Identification of the measured geometrical imperfections

The tank side surface imperfections can be considered in terms of a two-dimensional scalar random field described by a probability density function. In Wilde (1981) and Orlik (1976), the essential features of the measured imperfection fields were considered. The following hypotheses were formulated and proved:

- the stochastic process is stationary and ergodic along the horizontal lines,
- the random variables can be described by a Gaussian probability density function.

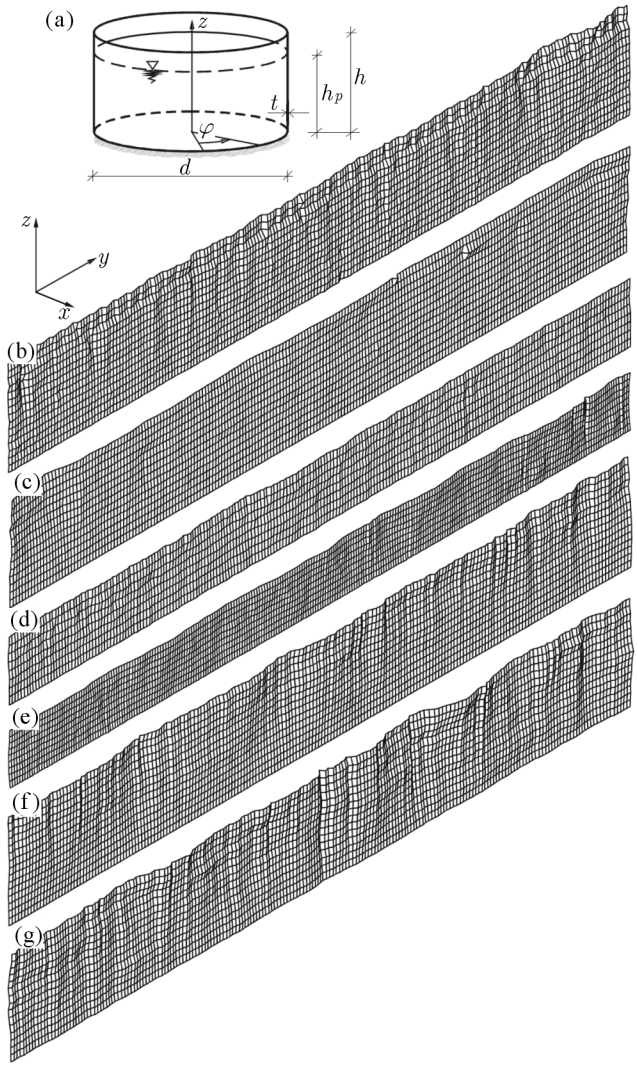

Fig. 1. Measured and simulated geometrical imperfections of petrol tanks. Notes: tanks are in different scales; in tanks no. 6 and no. 9 only every second vertical line is drawn. Measured imperfections: (b) tank no. 1 – $V = 5000\,\mathrm{m}^3$, $d = 23.75\,\mathrm{m}$, $h = 11.98\,\mathrm{m}$; (c) tank no. 3 – $V = 5000\,\mathrm{m}^3$, $d = 23.75\,\mathrm{m}$, $h = 11.98\,\mathrm{m}$; (d) tank no. 6 – $V = 30000\,\mathrm{m}^3$, $d = 49.50\,\mathrm{m}$, $h = 16.44\,\mathrm{m}$; (e) tank no. 9 – $V = 50000\,\mathrm{m}^3$, $d = 65.00\,\mathrm{m}$, $h = 18.01\,\mathrm{m}$. Simulated imperfection – tank no. 1: (f) estimation of measured imperfections – sample no. 1; (g) simulated extreme imperfections – sample no. 234

Table 2. Statistical description of measured initial geometrical imperfections of tanks

Tank no.	d [m]	Mean value $\overline{x}$ [m]	St. dev. σ_x [m]	$\lvert x_i^{max}\rvert$ [m]	$\overline{x}/d$	σ_x/d	$\lvert x_i^{max}\rvert/d$
1	11.875	$-0.763 \cdot 10^{-2}$	0.0233	0.159	$-0.643 \cdot 10^{-3}$	0.00197	0.0134
2	11.875	$-0.988 \cdot 10^{-2}$	0.0240	0.163	$-0.832 \cdot 10^{-3}$	0.00202	0.0137
3	11.875	$-0.485 \cdot 10^{-2}$	0.0153	0.110	$-0.408 \cdot 10^{-3}$	0.00129	0.00926
4	12.250	$-0.216 \cdot 10^{-1}$	0.0213	0.075	$-0.176 \cdot 10^{-2}$	0.00173	0.00612
5	17.790	$-0.994 \cdot 10^{-3}$	0.0329	0.139	$-0.559 \cdot 10^{-4}$	0.00185	0.00781
6	24.750	$-0.361 \cdot 10^{-2}$	0.0302	0.167	$-0.146 \cdot 10^{-3}$	0.00122	0.00675
7	24.750	$0.118 \cdot 10^{-1}$	0.0252	0.097	$0.476 \cdot 10^{-3}$	0.00101	0.00392
8	27.005	$0.297 \cdot 10^{-2}$	0.0278	0.108	$0.110 \cdot 10^{-3}$	0.00103	0.00400
9	32.500	$0.109 \cdot 10^{-2}$	0.0491	0.226	$0.334 \cdot 10^{-3}$	0.00151	0.00696

Using the above assumption, the following nonhomogeneous correlation function is introduced

$$K(y_1, y_2, z_1, z_2) = \alpha \frac{z_1 z_2}{h^2} \cos(\omega(y_2 - y_1)) \exp(-\beta|y_2 - y_1| - \gamma|z_2 - z_1|) \quad (2.1)$$

where: y_1, y_2, z_1, and z_2 are the point coordinates (see Fig. 1), α, ω, β, and γ are the correlation coefficients, and h denotes the tank height. The first term $\alpha z_1 z_2 h^{-2}$ determines a linear change of the standard deviation $\sigma_x = \sqrt{\alpha} z/h$ along the vertical line with zero value at the tank bottom and maximum at the top. The element $\cos(\omega(y_2 - y_1))$ assumes that the random variables permute along the perimeter according to the cosine function. The last term, $\exp(-\beta|y_2 - y_1| - \gamma|z_2 - z_1|)$, describes how fast the correlation between the neighbouring points vanishes in the horizontal and vertical directions.

The correlation function parameters α, ω, β, and γ are estimated on the basis of the measured data. Only the imperfection fields of tanks nos. 1-3 ($V = 5000\,\mathrm{m}^3$), no. 6 ($V = 30000\,\mathrm{m}^3$), and no. 9 ($V = 50000\,\mathrm{m}^3$) were measured using fine meshes (see Table 1). Thus, only five data sets were used to determine the constants of Eq. (2.1). The assumption that the random field of imperfections is ergodic along the horizontal lines makes it possible to analyse not a single (the measured) but hundreds of realizations. For example, in the first case (tank no. 1), as the imperfection values are given in 202 vertical lines, the same number of field realizations can be considered ($NR = 202$). For the reason that the imperfections were measured at 16 points along the vertical line, the dimension of the random vector $\boldsymbol{x}_i$ equals $16 \times 202 = 3232$. The global experimental covariance matrix $\mathbf{K}_e$ (size 3232×3232) of the

measured imperfection field was obtained according to the following statistical formulas

$$\mathbf{K}_e = \frac{1}{NR-1}\sum_{i=1}^{NR}(\boldsymbol{x}_i - \overline{\boldsymbol{x}})(\boldsymbol{x}_i - \overline{\boldsymbol{x}})^{\top}$$
$$\overline{\boldsymbol{x}} = \frac{1}{NR}\sum_{i=1}^{NR}\boldsymbol{x}_i \tag{2.2}$$

where $\boldsymbol{x}_i$ $(i = 1, \ldots, NR)$ is the measured imperfection vector, NR is the number of realizations, and $\overline{\boldsymbol{x}}$ represents the mean value vector.

Making use of the calculated matrix $\mathbf{K}_e$ (Eqs. (2.2)), the parameters of correlation function (2.1) are determined by a standard regression analysis. As any regression calculations concerning the global experimental covariance matrix size 3232×3232 are inefficient, only imperfections measured on limited areas of tank surfaces have been considered. In the cases of tanks nos. 1, 2 and 3, the random vectors $\boldsymbol{x}_i$ of dimensions 16×16 has been analysed. Similar reduction has been set up in the case of tanks nos. 6 and 9 (28×9 and 26×10, respectively). In the calculation, all horizontal lines are taken into considerations and only a limited number of the vertical lines. The magnitude of the reduced areas of the calculation are connected with the significant range of the correlation defined by (2.1). This simplification has reduced the time of regression analysis. The results – parameters of correlation function (2.1) – are presented in Table 3, in which the global G_{er} and variance V_{er} errors of the calculations are also presented. They are obtained using the following formulas

$$G_{er}(\mathbf{K}_e, \widehat{\mathbf{K}}_e) = \frac{\left|\|\mathbf{K}_e\| - \|\widehat{\mathbf{K}}_e\|\right|}{\|\mathbf{K}_e\|} \cdot 100\%$$
$$V_{er}(k_{ii}^e, \widehat{k}_{ii}^e) = \frac{1}{MN}\sum_{i=1}^{MN}\frac{k_{ii}^e - \widehat{k}_{ii}^e}{k_{ii}^e} \cdot 100\% \tag{2.3}$$

where $\|\mathbf{K}\| = \sqrt{\operatorname{tr}\mathbf{K}^2}$ is the matrix norm, k_{ii} denotes the diagonal element of the matrix, and MN describes the covariance matrix size. The elements of the covariance matrix estimator $\widehat{\mathbf{K}}_e$ were obtained by inserting the calculated correlation parameters in (2.1). The graphical representation of the selected experimental covariance matrix values $\mathbf{K}_e$ and their estimator $\widehat{\mathbf{K}}_e$, calculated with the help of the vector $\boldsymbol{x}_i$ defined on a 16×16 size mesh, is given in Fig. 2.

Table 3. Correlation parameters of covariance function (2.1)

Tank no.	Random vector $\boldsymbol{x}_i$ dimension	Correlation parameters of Eq. (2.1)				Errors	
		α	ω	β	γ	G_{er}	V_{er}
1	16×16	0.000716	0.317389	0.175900	0.058001	4.49	26.84
2	16×16	0.000707	0.329261	0.163659	0.050385	3.04	29.00
3	16×16	0.000533	0.421175	0.113103	0.098789	8.25	15.75
6	28×9	0.001397	0.154658	0.061831	−0.00861	1.84	22.21
9	26×10	0.005234	0.134896	0.040879	0.001564	0.78	6.40

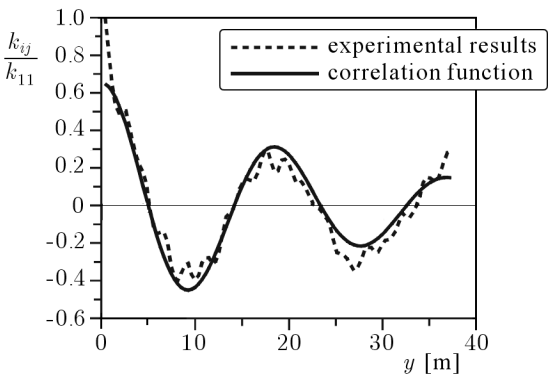

Fig. 2. Graphical representation of identified correlation matrix of imperfection field ($\boldsymbol{x}_i$ size equals 16×16); $y = 6.0\,\mathrm{m}$ (constant, half the shell height), $0 \leqslant x \leqslant 37.3\,\mathrm{m}$ (half the shell perimeter)

The error values and the plots show that the scattered pattern of imperfections was modelled accurately.

Analysing the results presented in Table 3, one can notice that only the first two sets of parameters describing the imperfections for tank no. 1 and no. 2 are similar. The results confirm the conclusions formulated above (see Table 2). It is obvious that the characteristics of geometrical imperfections vary depending on different tank dimensions. Also the difference between the tanks of the same capacity (tanks no. 1, no. 2 and no. 3) can be easily predicted. Comparing Fig. 1a,b, it is possible to notice that tank no. 3 was built much more precisely.

Similar calculations of the correlation coefficients can be made in the case of the limited measured data, i.e. for tanks nos. 4, 5, 7, and 8. For example, using the data of tank no. 4 (see Table 1), the following parameters have been obtained

$$\begin{aligned} \alpha &= 0.013612 \qquad & \omega &= 0.299437 \\ \beta &= 0.062983 \qquad & \gamma &= -0.009868 \end{aligned} \tag{2.4}$$

with the associated global and local errors: $G_{er} = 16.51\%$, $V_{er} = 4.48\%$. In this case, the calculations are performed with the help of all the available data (mesh 9×15, 128 measured points). Despite the fact that tank no. 4 ($V = 5000\,\mathrm{m}^3$) is almost identical to tanks 1-3, the results differ significantly (compare parameters (2.4) and those presented in Table 3). The differences result mainly from the limited data used in the calculations, i.e. 15 vertical lines in tank no. 4, and 202 when tank no. 1 is considered. The differences in the initial imperfection shapes and magnitudes (see Table 2) seem to have minor influence.

To indicate the effect of the number of measured imperfections on the correlation parameters, an additional simple analysis was performed. The measured data of tank no. 1 were reduced in such a way that their size was close to the data of tank no. 4, i.e. $8 \times 17 = 136$ points. On that basis, the following correlation parameters were estimated

$$\begin{aligned} \alpha &= 0.009893 \qquad & \omega &= 0.335382 \\ \beta &= 0.024198 \qquad & \gamma &= -0.013186 \end{aligned} \tag{2.5}$$

As expected, the results differ significantly from those obtained for the 16×202 measured points of tank no. 1 (see Table 3). Thus, the imperfection data for tanks 4, 7, 8, and 9 seem to be insufficient to describe the random fields properly. The method of identification of the imperfection fields on the basis of the limited data remained an open problem.

The analysis makes it possible to formulate the following conclusions:

- the number of the measuring points of imperfections should depend on the quality of the tank assembly,
- the data necessary for the acceptable definition of the random field of imperfections should be measured precisely, using a fine mesh, even when only a limited part of the tank (for example one quarter) is taken into consideration; measuring the entire tank side by a rough mesh gives inadequate results.

It is an important problem if a general rule can be established to describe the relation between the tank dimensions and the correlation coefficients. To this end, the parameter values (Table 3) are presented versus the tank diameters (see Fig. 3). Analysing the graph and taking into consideration the statistic data presented in Table 2, one can notice that the available data are too scattered to build a reliable general expression describing the random field of the tank imperfections. Only a draft formula can be estimated. For this purpose, the standard regression analysis is applied. The first coefficient α (Eq.

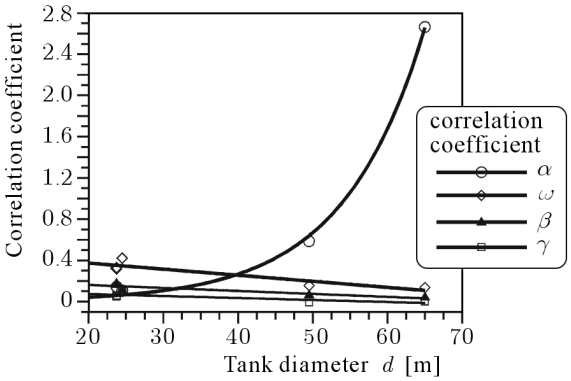

Fig. 3. Correlation coefficients (Eq. (2.1)) vs. tank diameter (see Table 4)

Table 4. Extreme values of geometrical imperfections

Tank no.	Extreme values		Tank edge
	z/h	x_{extr}/σ_x	x_{extr}/σ_x
1	0.0625	4.5511	3.6533
2	0.1250	4.5764	3.5357
3	0.7333	3.8638	3.3294
4	0.3750	2.3853	1.6780
5	0.8571	2.5232	2.3843
6	1.0000	3.6732	3.6732
7	1.0000	2.6984	2.6984
8	0.0625	3.3931	2.4055
9	0.1000	4.7730	2.8431
The means:		3.6042	2.9112

(2.1)) is described with the help of an exponential function, and the coefficients ω, β and γ are defined by straight lines (see Fig. 3)

$$\begin{aligned} \alpha &= 0.006733 \exp(0.091963d) \\ \omega &= -0.005894d + 0.491321 \\ \beta &= -0.002876d + 0.218356 \\ \gamma &= -0.001931d + 0.112063 \end{aligned} \tag{2.6}$$

where d is the tank diameter.

Formulas (2.6) can be improved when new data are included in the calculations (Kowalski, 2004). Further improvements can be obtained describing the correlation coefficients as functions of standard deviations of imperfections and their extreme values.

2.2. Envelope of tank geometrical imperfections

It is possible to describe the correlation function as an envelope of the extreme imperfections. For this purpose, the standard deviations of tank imperfections for each horizontal level are calculated. The obtained normalized standard deviations for all tank data are plotted in Fig. 4. Examining these data, it is easy to notice that the tank side imperfections start from the bottom, and their values indicate the same order as the imperfections measured at higher levels. Therefore, the simplest solution is the approximation of the standard deviation to a parabolic function

$$\sigma = \sqrt{\alpha z} h \tag{2.7}$$

Then, the correlation function of the imperfection field takes the form

$$K(y_1, y_2, z_1, z_2) = \alpha \sqrt{\frac{z_1 z_2}{h}} \cos(\omega(y_2 - y_1)) \exp(-\beta|y_2 - y_1| - \gamma|z_2 - z_1|) \tag{2.8}$$

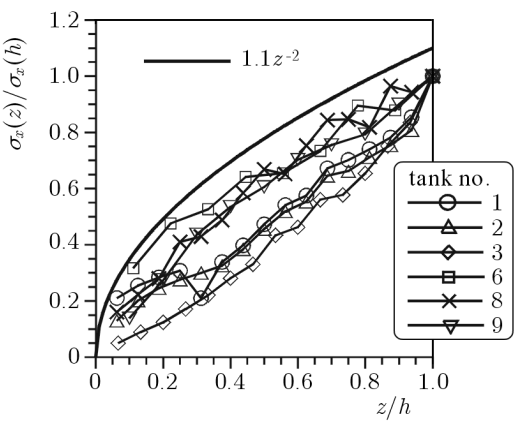

Fig. 4. Normalized standard deviations of geometric imperfections calculated separately for each level

The coefficient α is evaluated in such a way that the standard deviation value at the top of the tank is increased by 10%. For example, in the case of tank no. 1 $\sqrt{\alpha} = 0.0364$. The other correlation parameters ω, β, and γ (see Eq. (2.8)) remain unchanged (Table 3). The normalized envelope for all tank data is presented in Fig. 4. The results have proved that the adopted envelope in the parabolic shape describes precisely possible extreme imperfections.

Proposed correlation functions (2.1) and (2.8), and the estimated values of the parameters α, ω, β, and γ make it possible to simulate vertical geometrical imperfections of the tank.

3. Simulation of geometrical imperfections

The simulation process is presented using the data of tank no. 1 (Table 1). Two cases are analysed, i.e. simulation of the measured imperfections as precisely as possible, and simulation of the maximal imperfection values.

The field of imperfections is numerically simulated taking advantage of correlation function (2.1) and the estimated constants presented in Table 3. In the process, the conditional-rejection simulation method is used (see Bielewicz *et al.*, 1994; Walukiewicz *et al.*, 1997; Górski, 2006). This technique has been successfully applied to spatial descriptions of soil random properties (Przewłócki and Górski, 2001; Tejchman and Górski, 2006) and to environmental problems (Jankowski and Walukiewicz, 1997). Here, only a brief description of this method is presented.

3.1. Conditional-rejection simulation method

A discrete random field can be described by multidimensional random variables defined at mesh nodes. The field is represented by the random vector $\boldsymbol{x}_{(m\times 1)}$ and its mean value $\overline{\boldsymbol{x}}_{(m\times 1)}$. The correlation function is replaced by the symmetric and positively defined covariance matrix $\mathbf{K}_{(m\times m)}$. The random variable vector $\boldsymbol{x}_{(m\times 1)}$ is divided into blocks consisting of the unknown $\boldsymbol{x}_{u(n\times 1)}$ and the known $\boldsymbol{x}_{k(p\times 1)}$ elements $(n+p=m)$. The covariance matrix $\mathbf{K}_{(m\times m)}$ and the expected values vector $\overline{\boldsymbol{x}}_{(m\times 1)}$ are also appropriately cut

$$\boldsymbol{x} = \begin{Bmatrix} \boldsymbol{x}_u \\ \boldsymbol{x}_k \end{Bmatrix}_{(n+p)} \qquad \mathbf{K} = \begin{bmatrix} \mathbf{K}_{11} & \mathbf{K}_{12} \\ \mathbf{K}_{21} & \mathbf{K}_{22} \end{bmatrix}_{(n+p)\times(n+p)} \qquad \overline{\boldsymbol{x}} = \begin{Bmatrix} \overline{\boldsymbol{x}}_u \\ \overline{\boldsymbol{x}}_k \end{Bmatrix}_{(n+p)} \tag{3.1}$$

The unknown vector $\boldsymbol{x}_u$ is estimated from the following conditional truncated distribution (Jankowski and Walukiewicz, 1997)

$$f_t\Big(\frac{\boldsymbol{x}_u}{\boldsymbol{x}_k}\Big) = \frac{1}{[(1-t)2\pi]^m \det \mathbf{K}_c} \exp\Big(-\frac{1}{2(1-t)}(\boldsymbol{x}_u - \overline{\boldsymbol{x}}_c)^\top \mathbf{K}_c^{-1}(\boldsymbol{x}_u - \overline{\boldsymbol{x}}_c)\Big) \tag{3.2}$$

where $\mathbf{K}_c$ and $\overline{\boldsymbol{x}}_c$ are described as the conditional covariance matrix and conditional expected value vector

$$\begin{aligned} \mathbf{K}_c &= \mathbf{K}_{11} - \mathbf{K}_{12}\mathbf{K}_{22}^{-1}\mathbf{K}_{21} \\ \overline{\boldsymbol{x}}_c &= \overline{\boldsymbol{x}}_u + \mathbf{K}_{12}\mathbf{K}_{22}^{-1}(\boldsymbol{x}_k - \overline{\boldsymbol{x}}_k) \end{aligned} \tag{3.3}$$

The constant t is the truncation parameter

$$t = \frac{s \exp(-s^2/2)}{\sqrt{2\pi}\,\mathrm{erf}\,(s)} \tag{3.4}$$

The constant s (Eq. (3.4)) is usually related to the standard deviation of the random field points.

The random vector of the unknown variables $\boldsymbol{x}_u$ is simulated using the rejection method (Devroye, 1986). The single random points of the vector $\boldsymbol{x}_u$ are generated according to the following formula

$$x_i = a_i + (b_i - a_i)u_i \qquad i = 1, \ldots, m \tag{3.5}$$

where u_i denotes the random variables uniformly distributed in the interval $[0, 1]$, and (a_i, b_i), $i = 1, 2, \ldots, m$ are the intervals of the reals. The value x_i is generated according to (3.5) to fulfil condition (3.2) (the trial and error method). The intervals a_i and b_i are defined for all points of the mesh and establish an envelope of the random field. The envelope specifies the characteristic features of the field under consideration, for example, the maximal and minimal values and the field boundary conditions. It can be given in the form of a function or by experimental discrete data.

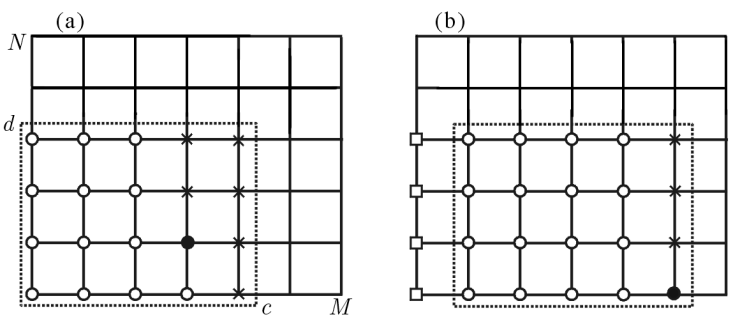

Fig. 5. Simulation process – coverage of field points with moving propagation scheme; ○ – known values, ● – simulated value, × – unknown values simulated in one base scheme step, □ – known values not included in base scheme calculations

The direct application of the rejection method is inefficient. To improve it, a base scheme of random values is defined (Bielewicz *et al.*, 1994). The scheme is placed at the nodal points of the mesh in such a way that it covers all the nodes i, $1 \leqslant i \leqslant m$, $m = M \times N$ (Fig. 5). The simulation process is divided into three stages. First, four-corner random values are simulated. Next, the propagation scheme with a growing number of points covers the

defined base scheme of the field mesh. In the example shown in Fig. 5a the dimension of the base scheme equals $c \times d = 5 \times 5 = 20$ random values (mesh points). In the third stage, the base scheme is appropriately shifted, and the next group of unknown random values is simulated (see Fig. 5b). The base scheme is translated so as to cover all the field nodes. As the simulated field of tank imperfections is a form of circular data, the algorithm has been improved. When the calculations along the circle (the horizontal lines) are being closed, the base scheme is modified accordingly.

The base scheme and the random field envelope are the characteristic features of the conditional-rejection simulation method. They make it possible to simulate the fields describing any two-dimensional shapes (three dimensional problems can also be analysed). The size of the field is practically unlimited (a thousand of mesh points).

3.2. Simulation of measured and extreme tank imperfections

According to the method of simulation, the random field envelope – i.e. the lower a_i and the upper boundary b_i (see Eq. (3.5)) – have to be defined for each mesh point i. The parameters determine the theoretical maximal and minimal values of imperfections and should be related to their standard deviations. Since the imperfection field is assumed to be ergodic, the same boundary values are assigned to each horizontal line. To estimate them, the imperfection mean values and the standard deviations calculated separately for all horizontal lines are analysed once more. The extreme imperfections related to their standard deviations are presented in Table 4. They appear on different tank levels (z/h in Table 4). Only in two cases the extreme values occurred on the tank edges (tank no. 6 and 7). The maximal value $x_{extr}/\sigma_x = 4.7730$ appeared in tank no. 9 ($V = 50000\,\mathrm{m}^3$). Analysing the data, the following values describing the random field boundary have been assumed

$$a_i, b_i = \pm s\sigma_i = \pm 5\sigma_i \tag{3.6}$$

where σ_i is the standard deviation at the point i (see Eq. (2.1))

$$\sigma_i^2 = K(y_i, y_i, z_i, z_i) = \alpha \frac{z_i^2}{h^2} \tag{3.7}$$

The next simulation parameter, i.e. the simulation base scheme (see Fig. 5) is defined as a rectangle of dimension 16×16 points. This base scheme is moved horizontally step by step to cover all mesh points. The procedure allows for simulating the tank imperfections, i.e. along the cylindrical surface. As many

as 2000 realizations have been simulated. Using formulae (2.3), the following errors in the field simulation have been found

$$G_{er} = 3.30\% \qquad V_{er} = 3.48\% \tag{3.8}$$

Values (3.8) indicate excellent convergence of the field estimators. Additionally, samples no. 1 of the simulated field of imperfections is presented in Fig. 1f. It can be noticed that the essential features of the measured imperfection map have been numerically reproduced.

The same calculation can be performed in order to obtain the extreme geometrical imperfection field. For this purpose, Eq. (2.8) with the following correlation coefficients

$$\begin{aligned} \sqrt{\alpha} &= 0.0364 & \omega &= 0.317389 \\ \beta &= 0.175900 & \gamma &= 0.058001 \end{aligned} \tag{3.9}$$

is implemented.

The same boundary values (3.6) are used. After simulating 2000 realizations, the following errors occurred

$$G_{er} = 0.15\% \qquad V_{er} = 0.41\% \tag{3.10}$$

A sample of the simulated initial imperfection vector is presented in Fig. 1g. The mean value of the vector characterizes the extreme value chosen from all 2000 samples in the set. Thus, the sample is an extreme one (in the defined sense).

4. Numerical calculation of vertical petrol tank

The preliminary numerical calculations include three cases of tank no. 1 ($5000\,\mathrm{m}^3$).

The first case refers to an ideal cylindrical shell whose data are presented in Fig. 1a (Orlik, 1976). The tank is made of 6 strakes of plates, each ca. 2000 mm in height, and of thicknesses $t = 11$, 10, 8, and 7 mm, starting from the bottom. Steel St3VY is used for the lower side plates and the first row of the bottom plates, and steel St3SY for other plates. The steel yield stress has been assumed to be $R = 255\,\mathrm{MPa}$. The petrol level, of specific gravity $\rho = 50\,\mathrm{MN/m}^3$, is raised in every incremental step (its maximal value $h_p = 11.25\,\mathrm{m}$). Other data of the tank, for example, the soil (foundation) parameters $k = 50\,\mathrm{MN/m}^3$,

are taken from Ziółko (1986). 15646 finite elements were used for the tank model mesh (Górski and Mikulski, 2005). Some of the results, obtained with the help of MSC NASTRAN (MSC Nastran for Windows, 2001), are presented in Table 5.

Table 5. Extreme stresses, bending moments and axial forces in tanks with and without initial geometrical imperfections

Internal forces	Tank surface		
	Ideal	Measured imperfections	Simulated imperfections
Maximal stresses σ_R [MPa]	92.24	255	255
Bending moments m_z [kNm/m]	−0.67-0.98	−2.51-4.19	−1.38-3.76
Bending moments m_φ [kNm/m]	−0.20-0.29	−4.11-2.68	−3.42-2.40
Axial force n_z [kN/m]	−7.97-20.56	−516.1-335.7	−712.7-448.2
Axial force n_φ [kN/m]	−1.23-1025.0	−433.6-1319.0	−945.2-1227.0

The tank data for the second case include measured initial geometrical imperfections presented in Fig. 1b (Orlik, 1976). As the imperfections refer only to 16 horizontal and 202 vertical lines (3232 points), the missing mesh values are determined by linear interpolation using the neighbouring data. The basis of the numerical calculation is the deformed shape of the cylindrical tank assumed to be stress free. The results are presented in Table 5.

The third calculation is performed for the simulated extreme imperfections shown in Fig. 1g.

The results of nonlinear calculations (see Table 5) indicate that the tank initial imperfections can cause significant variations in stress fields in comparison with the solution related to an ideal surface. The steel of the tank with imperfections yields at a point connecting the bottom with the side plates and in areas of extreme imperfections. It should be noted that the yielding process occurrs despite the fact that the initial field of imperfections is rather a typical one (see Fig. 1b).

5. Conclusions

On the basis of the presented analysis, the following comments and suggestions having reference to future improvements of the identification and modelling of the random fields of imperfections in tanks can be made:

- A method of measuring geometrical imperfections in tanks should be formulated. It is essential to define the minimal tank area and the size

of the mesh of measuring points. It has been shown that the parameters depend on the tank diameter as well as characteristics and magnitude of the imperfections.

- A generalized version of the correlation function should be formulated for steel cylindrical tanks of various dimensions. The presented primary relations can help in future improvements when more measured data can be incorporated in the estimation.

- The procedure of identification of the correlation function from limited data measured in situ needs further investigation.

- The achieved results, aided by the statistical analysis, have proved the capability of the conditional-rejection method to precisely simulate geometrical imperfections in tanks when the correlation function is known.

- The random numerical model of tanks can be easily extended, for example, by introducing random variability of soil foundations which can have a degrading effect on the tank loading capacity.

- The presented results of numerical calculations have revealed that the initial geometrical imperfections have influence on the mechanical behaviour of steel cylindrical tanks. Formulation of a methodology of identification, classification and description of the tank imperfections can lower the laborious and high cost of experiments and ensure a better and much safer design.

Designing a new tank, the correlation function and the appropriate standard deviations of the geometric imperfections can be described according to the measured data of existing tanks of similar dimensions. Then, the simulation procedure can be applied and, from the simulated set, some extreme realizations can be selected. The selection criteria of characteristic samples are, for example: the extreme value of imperfections, norms of the imperfection vectors, the number of sign changes (number of waves) along the horizontal lines. On the basis of the selected extreme samples, it is possible to calculate stress fields of the structure. In this way, the most dangerous stress state related to all simulated but realistic data can be obtained. A definition of the critical state of a steel petrol tank should also be established. Usually, plastic deformation of the tank side is considered dangerous as steel becomes brittle. Cyclic loading conditions of the tank also play an important role in the definition of the critical state.

References

1. ANDERS M., HORI M., 1999, Stochastic finite element method for elasto-plastic body, *International Journal for Numerical Methods in Engineering*, **46**, 1897-1916
2. ARBOCZ J., 1998, On accuracy of numerical buckling load predictions, *Proc. of the 6th Conference "Shell Structures. Theory and Applicatios"*, Gdańsk-Poland, 19-23
3. ARBOCZ J., STARNES J.H., 2002, Future directions and challenges in shell stability analysis, *Thin-Walled Structures*, **40**, 729-754
4. AUGUSTI G., BARATTA A., CASCIATI F., 1984, *Probabilistic Methods in Structural Engineering*, London, New York: Chapman and Hall
5. BENDAT J.S., PIERSOL A.G., 1993, *Engineering Applications of Correlation and Spectral Analysis*, New York: John Wiley & Sons
6. BIELEWICZ E., GÓRSKI J., 2002, Shell with random geometric imperfections. Simulation-based approach, *International Journal of Non-linear Mechanics*, **37**, 4/5, 777-784
7. BIELEWICZ E., GÓRSKI J., SCHMIDT R., WALUKIEWICZ H., 1994, Random fields in the limit analysis of elastic-plastic shell structures, *Computers and Structures*, **51**, 3, 267-275
8. BRANDT S., 1997, *Statistical and Computational Methods in Data Analysis*, New York: Springer Verlag
9. DEVROYE L., 1986, *Non-Uniform Random Variate Generation*, New York: Springer-Verlag
10. FERSON S., GINZBURG L.R., 1996, Different methods are needed to propagate ignorance and variability, *Reliability Engineering and System Safety*, **54**, 133-144
11. FISHER N.I., 1993, *Statistical Analysis of Circular Data*, Great Britain, Cambridge University Press
12. GÓRSKI, J., 2006, Non-linear models of structures with random geometric and material imperfections simulation-based approach, *Gdansk University of Technology, Monograph*, **68**
13. GÓRSKI J., MIKULSKI T., 2005, Statistical description and numerical calculations of cylindrical vertical tanks with initial geometric imperfections, *Proc. of the 7th International Conference Shell Structures. Theory and Applications*, Gdańsk Jurata 2005; London: Balkema, Taylor & Francis, 547-551
14. HURTADO J.E., BARBAT A.H., 1998, Monte Carlo techniques in computational stochastic mechanics, *Archives of Computational Method in Engineering*, **5**, 1, 3-30

15. JANKOWSKI R., WALUKIEWICZ H., 1997, Modeling of two-dimensional random fields, *Probabilistic Engineering Mechanics*, **12**, 2, 115-121

16. KHAMLICHI A., BEZZAZI M., LIMAM A., 2004, Buckling of elastic cylindrical shells considering the effect of localized axisymmetric imperfections, *Thin-Walled Structures*, **42**, 1035-1047

17. KOWALSKI D., 2004, Influence of initial imperfections on the vertical tank side stresses, Ph.D. Thesis. Gdańsk University of Technology, Gdańsk [in Polish]

18. LI C.C., DER KIUREGHIAN A., 1993, Optimal discretization of random fields, *Journal of Engineering Mechanics*, **119**, 6, 1136-1154

19. MAREK P., GUŠTAR M., ANAGNOS T., 1996, *Simulation-Based Reliability Assessment for Structural Engineers*, New York, London, Tokyo: CRC Press, Boca Raton

20. MATTHIES H.G., BRENNER C.E., BUCHER C.G., SOARES C.G., 1997, Uncertainties in probabilistic numerical analysis of structures and solids – stochastic finite elements, *Structural Safety*, **19**, 3, 283-336

21. MELCHERS R.E., 1999, *Structural Reliability Analysis and Prediction*, Chichester: John Wiley & Sons

22. MIGNOLET M.P., SPANOS P.D., 1992, Simulation of homogeneous two-dimensional random fields: Part I – AR and ARMA models, *Journal of Applied Mechanics, ASME*, **59**, 2, 260-269

23. MSC Nastran for Windows, 2001, Los Angeles: MSC Software Corporation

24. ORLIK G., 1976, Deformation of shapes of cylindrical steel shells, statistical analysis and numerical simulations, Ph.D. Thesis. Technical University of Gdańsk, Gdańsk [in Polish]

25. PAPADIMITRIOU C., BECK J.L., KATAFYGIOTIS L.S., 2001, Updating robust reliability using structural test data, *Probabilistic Engineering Mechanics*, **16**, 103-113

26. PAPADOPOULOS V., PAPADRAKAKIS M., 2004, Finite-element analysis of cylindrical panels with random initial imperfections, *Journal of Engineering Mechanics*, **130**, 8, 867-876

27. PRZEWŁÓCKI J., GÓRSKI J., 2001, Strip foundation on 2-D and 3-D random subsoil, *Probabilistic Engineering Mechanics*, **16**, 2, 121-136

28. RAIZER V., 2004, Theory of reliability in structural design, *Applied Mechanical Review*, **57**, 1, 1-21

29. SCHENK C.A., SCHUËLLER G.I., 2003, Buckling analysis of cylindrical shells with random geometric imperfection, *International Journal of Non-Linear Mechanics*, **38**, 1119-1132

30. SCHUËLLER G., 2001, Computational stochastic mechanics – recent advances, *Computers and Structures*, **79**, 2225-2234

31. SPANOS P.D., MIGNOLET M.P., 1992, Simulation of homogeneous two-dimensional random fields: Part II – MA and ARMA models, *Journal of Applied Mechanics, ASME*, **59**, 2, 270-277

32. STEFANOU G., PAPADRAKAKIS M., 2004, Stochastic finite element analysis of shells with combined random material and geometric properties, *Computer Methods in Applied Mechanics and Engineering*, **193**, 139-160

33. SURDET B., DER KIUREGHIAN A., 2002, Comparison of finite element reliability methods, *Probabilistic Engineering Mechanics*, **17**, 337-348

34. TEJCHMAN J., GÓRSKI J., 2006, Stochastic FE-analysis of shear localization in 2D granular material within a micro-polar hypoplasticity, *Archives of Hydro-Engineering and Environmental Mechanics*, **53**, 4, 1231-3726

35. VANMARCKE E., 1983, *Random Fields: Analysis and Synthesis*, Cambridge: MIT Press

36. VANMARCKE E., SHINOZUKA M., NAKAGIRI S., SCHUËLLER G.I., GRIGORIU M., 1986, Random fields and stochastic finite elements, *Structural Safety*, **3**, 143-166

37. WALUKIEWICZ H., BIELEWICZ E., GÓRSKI, J., 1997, Simulation of nonhomogeneous random fields for structural applications, *Computers and Structures*, **64**, 1/4, 491-498

38. WILDE P., 1981, *Random Fields Discretization in Engineering Calculations*, Warsaw: PWN, [in Polish]

39. ZHANG J., ELLINWOOD B., 1995, Error measure for reliability studies using reduced variable set, *Journal of Engineering Mechanics, ASCE*, **121**, 8, 935-937

40. ZIÓŁKO J., 1986, *Metal Tanks for Liquids and Gases*, Warsaw: Arkady [in Polish]

Identyfikacja i symulacja wstępnych imperfekcji geometrycznych w stalowych cylindrycznych zbiornikach

Streszczenie

Wyznaczenie obciążenia granicznego konstrukcji powłokowych wymaga uwzględnienia w obliczeniach odchyłek geometrycznych. Wykonanie pomiarów tego typu odchyłek rzeczywistych obiektów jest trudne i kosztowne. Wyniki uzyskane na podstawie analizy modeli laboratoryjnych nie są wiarygodne. W pracy zaproponowano metodę alternatywną. Wykazano, że na podstawie dostępnych danych można sformułować

metody identyfikacji i symulacji wstępnych odchyłek geometrycznych. Zaprezentowane procedury umożliwiają odwzorowanie pomierzonych pól wstępnych odchyłek stalowych cylindrycznych zbiorników o osi pionowej na paliwa płynne. Symulacje niejednorodnych pól losowych imperfekcji wykonano za pomocą oryginalnej warunkowej metody akceptacji i odrzucania. Pomierzone dane pozwoliły także na wyznaczenie obwiedni odchyłek losowych i na tej podstawie wykonano symulację ekstremalnych, realistycznych pól imperfekcji. Dodatkowo przeprowadzono nieliniowe obliczenia numeryczne zbiorników idealnych oraz z imperfekcjami. Porównanie wyników pozwoliło na określenie wpływu odchyłek na mechaniczną odpowiedź powłoki.

Manuscript received May 21, 2007; accepted for print November 14, 2007